# The Superchair : A Holonomic Omnidirectional Wheelchair with a Variable Footprint Mechanism

**Haruhiko H. Asada**
Principal Investigator

**Masayoshi Wada**
Visiting Scientist

## Abstract

A reconfigurable mechanism for varying the footprint of a four-wheeled omnidirectional vehicle is developed and applied to wheelchairs. The variable footprint mechanism consists of a pair of beams intersecting at a pivotal point in the middle. Two pairs of ball wheels at the diagonal positions of the vehicle chassis are mounted, respectively, on the two beams intersecting in the middle. The angle between the two beams varies actively so that the ratio of the wheel base to the tread may change. Four independent servomotors driving the four ball wheels allow the vehicle to move in an arbitrary direction from an arbitrary configuration as well as to change the angle between the two beams and thereby change the footprint. The objective of controlling the beam angle is threefold. One is to augment static stability by varying the footprint so that the mass centroid of the vehicle may be kept within the footprint at all times. The second is to reduce the width of the vehicle when going through a narrow doorway. The third is to apparently change the gear ratio relating the vehicle speed to individual actuator speeds. First the concept of the varying footprint mechanism is described, and its kinematic behavior is analyzed, followed by the three control algorithms for varying the footprint. A prototype vehicle for an application of wheelchair platform is designed, built, and tested.



**d'Arbeloff Laboratory for Information Systems and Technology**
**MIT**

# 1. Introduction

A holonomic omnidirectional vehicle is a highly maneuverable vehicle that can move in an arbitrary direction from an arbitrary configuration. Unlike traditional nonholonomic vehicles, the holonomic vehicle can move in an arbitrary direction continuously without changing the direction of the wheels. It can move back and forth, slides sideways, and rotates at the same position. Therefore the holonomic vehicle would be useful for wheelchairs, which need to maneuver in crowded locations such as residential homes, hospitals and long-term care units as well as factories.

In the past decades, a variety of holonomic omnidirectional vehicles have been developed. The Swedish Wheel[1] is the first to accomplish omnidirectional motion without changing the direction of the wheels. The Swedish Wheel has been applied to a wheelchair[2] and other applications[3]. Pin and Killough developed a unique omnidirectional vehicle with powered wheel units consisting of a pair of round wheels that alternately touch the floor[4]. The Omni-Track with ball wheels arranged in a crawler mechanism allows for sideway motion with large traction forces[5]. The VUTON omnidirectional vehicle consisting of arrays of cylindrical tires combined with an unique crawler mechanism is capable of carrying a large payload[6]. The Ball Wheel omnidirectional vehicle developed by the authors' group uses spherical tires held by a novel ring roller mechanism that transmits an actuator torque to the ball wheel[7]. This Ball Wheel Vehicle exhibits smooth motion with no shimmy and jerk along with highly maneuverable and precise movements, all of which are desirable features for wheelchair applications.

To apply the Ball Wheel to a wheelchair, however, the vehicle must meet several requirements for complex indoor applications. First, the vehicle body must be compact enough to go through narrow doorways. Standard doors are limited in width; the vehicle's tread and chassis width must confirm to the dimensional constraints. A narrow tread, however, may incur instability of the vehicle. As the patient moves, the mass centroid of the vehicle may shift in a wide range. Moreover, infirm patients cannot sit up in the middle of the chair, but tend to lean towards the arm rests. The footprint of the wheelchair[1] must be wide enough to prevent the patient from falling on the floor. A large footprint is therefore desirable for stability and safety, while wheelchairs must conform to dimensional constraints. Also the footprint must be compact since a large footprint does not allow the vehicle to maneuver in a closely confined place. Stability and maneuverability are therefore conflicting requirements.

[1] In this paper, footprint refers to the area enclosed by the contact points of the vehicle wheels.

Traditional vehicle designs with fixed footprint configurations would not provide an efficient solutions to this stability-maneuverability trade-off problem.

In addition, the original Ball Wheel Vehicle has three wheels to achieve 3 DOF motion. Its footprint is a triangular area, which is inadequate for maintaining stability. A four-wheeled vehicle is desirable, but incurs an over constraint problem between the active wheels and the ground since the vehicle has only three DOF while the four motors drive the four wheels independently. The over constraint problem may result in slip at the wheels or generate unwanted internal forces within the vehicle chassis.

In this paper, a novel reconfigurable footprint mechanism will be developed to augment stability and enhance maneuverability as well as to resolve the over-constraint problem. This new mechanism would allow to vary the ratio of wheel base to tread so that the vehicle could go through a narrow doorway and that the mass centroid could be kept within the footprint at all times. Furthermore, this varying footprint mechanism would function as a kind of continuously varying transmission (CVT) that changes the gear ratio between the actuator speed and the resultant vehicle speed. Therefore, the vehicle would be able to meet diverse requirements for speed and torque, exhibiting enhanced maneuverability and efficiency. In the following sections, the new mechanism will be described together with the original ball wheel mechanism. Its kinematic and static behavior will be analyzed, and algorithms for stability augmentation and transmission control will be developed. Experiments by using a prototype vehicle will be presented at the end to demonstrate the feasibility and validity of the proposed method.

## 2. Mechanical Design

### 2.1 The Ball Wheel Mechanism[7]

The Ball wheel mechanism with a special roller ring, shown in Figure 1-(a), is used for the vehicle. The ball is held by roller ring *A* at a great circle together with a set of bearings *B* arranged on another great circle. The roller ring is rotated by a servo motor to drive the ball wheel. Since the ring is inclined, a traction force is created between the ball wheel and the floor, as shown in the plane view, Figure1-(b). The stationary bearings *B*, arranged on the second great circle, allow passive rotation of the ball about an arbitrary axis within that great circle. As a result, the ball is free to move in the

direction perpendicular to the traction force, as shown in Figure 1-(b). The vehicle must have at least three ball wheels, each generating a traction force in a different direction. The resultant force acting on the vehicle is given by the vectorial sum of the traction forces. Varying the combination of the traction forces creates an arbitrary force and moment driving the vehicle.

The vehicle consisting of these ball wheels can move in an arbitrary direction with an arbitrary linear velocity and rotational velocity at an arbitrary position and orientation. There is no singular point in this mechanism, hence it is omnidirectional and holonomic. Moreover, this ball wheel vehicle allows for smooth motion with no shimmy and jerk, all of which are desirable for wheelchairs transporting patients.

### 2.2 A Reconfigurable Footprint Mechanism

Figure 2 shows the schematic of a new reconfigurable footprint mechanism for a four-wheeled holonomic omnidirectional vehicle. All the wheels are the ball wheels described above with independent suspensions. Two pairs of the ball wheels at diagonal positions are fixed to the tips of two beams intersecting at a pivotal joint in the middle. The two beams rotate about this pivotal joint so that the ratio of wheelbase to tread can vary. To go through a narrow doorway, the tread becomes narrow while the wheelbase becomes long, as shown in Figure 3-(a). To increase sideway stability, the tread is expanded, as shown in Figure 3-(c). To be isotropic, the two beams intersect at the right angle, as shown in Figure 3-(b).

One design issue with this reconfigurable footprint mechanism is that the chair mounted on the vehicle must be kept aligned with the bisector of the two beams intersecting at the pivotal joint, although both beams rotate about the joint. To this end, a differential gear mechanism is used for the pivotal joint. As shown in Figure 4, the three bevel gears form a differential gear mechanism. The middle bevel gear, Gear 3, rotates freely about the horizontal shaft $\beta$ that is fixed to the vertical shaft $\alpha$. Bevel gear 1 is fixed to beam *A*, while bevel gear 2 to beam *B*. When beam *A* rotates about the vertical shaft $\alpha$ together with bevel gear 1, bevel gear 3 rotates. As a result, bevel gear 2 rotates the same amount but in the opposite direction to bevel gear 1. In consequence, the chair mounted on the vertical shaft $\alpha$ is kept at the bisector position of the intersecting beams, *A* and *B*. The angle between the two beams is measured by a potentiometer, as shown in the figure.

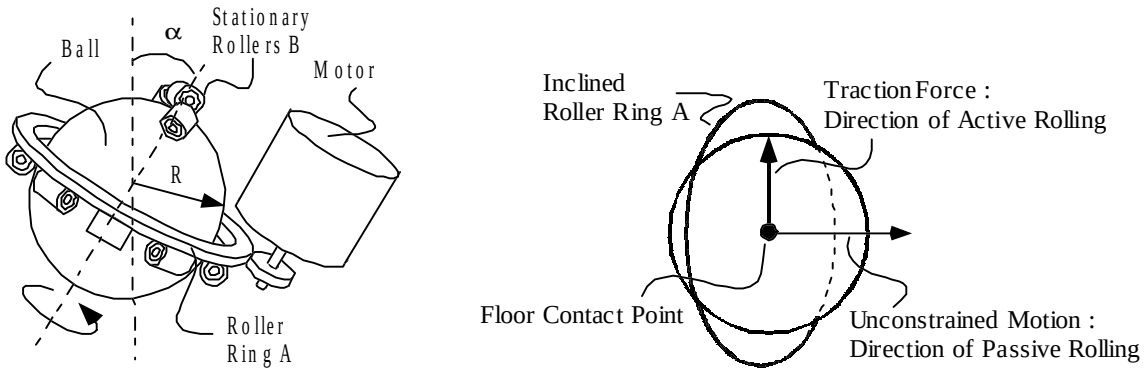


(a) Ball wheel unit (b) Plane view seen from the top of the ball wheel

Figure 1: Ball wheel mechanism

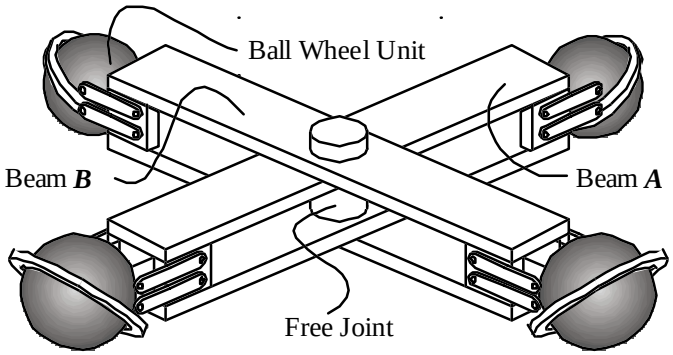


Figure 2: Omnidirectional reconfigurable vehicle

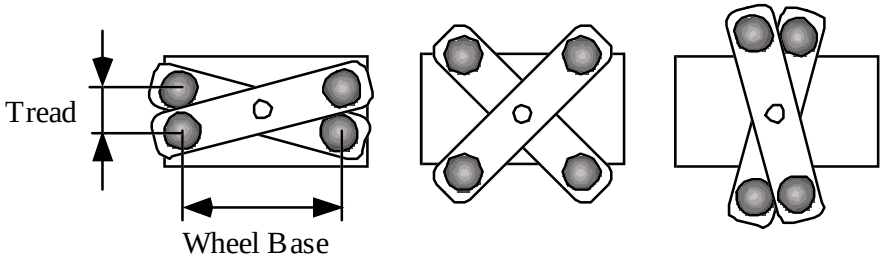


(a)narrow configuration (b)isotropic configuration (c)wide configuration

Figure 3: Reconfiguration of the footprint of the vehicle

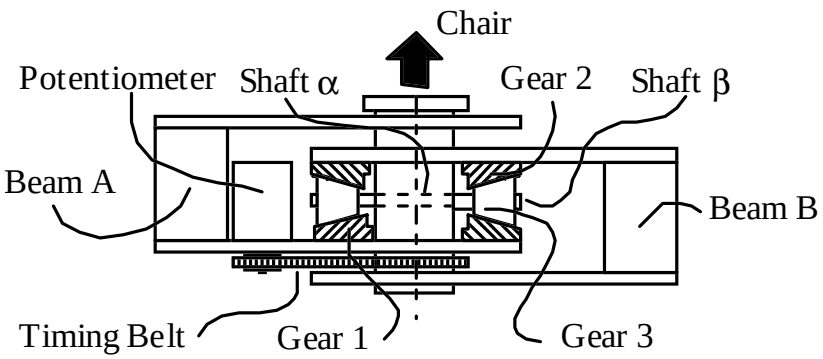


Figure 4: Pivotal joint of the vehicle

## 3. Kinematic Analysis

### 3.1 Ball Wheel

Consider the *i*-th ball wheel and half the beam holding the ball wheel, as shown in Figure 5. As ball rolls on the floor, i.e. the X-Y plane, the contact point with the X-Y plane moves together with the beam. The time rate of change of the contact point is called ball velocities, $v_{xi}$ and $v_{yi}$, with reference to the fixed frame O-XY. The pivotal joint of the vehicle, denoted $O_v$ in the figure, moves at $v_{xv}$ and $v_{yv}$ and the angular velocity of the i-th half beam is denoted $\phi_i$. The ball velocities, $v_{xi}$ and $v_{yi}$, are given by

$$\begin{bmatrix} v_{xi} \\ v_{yi} \end{bmatrix} = \begin{bmatrix} 1 & 0 & -L\sin\phi_i \\ 0 & 1 & L\cos\phi_i \end{bmatrix} \begin{bmatrix} v_{xv} \\ v_{yv} \\ \dot{\phi}_i \end{bmatrix} \qquad (1)$$

where $L$ is the distance between the pivotal joint $O_v$ and the contact point of the ball wheel. The ball wheel rolls in one direction, and is free to roll in the direction perpendicular to the active direction, as mentioned in section 2.1. Let $\psi$ be the angle pointing in the direction of active rolling on the O-XY plane, as shown in Figure 5. Note that $\psi$ is measured relative to the beam to which the ball wheel unit is fixed. The ball velocities, $v_{xi}$ and $v_{yi}$, can be decomposed into the velocity in the active direction, $v_{ai}$, and the one in the passive direction. Using eq.(1), the active velocity component $v_{ai}$ is given by

$$v_{ai} = v_{xi}\cos(\phi_i + \psi) + v_{yi}\sin(\phi_i + \psi)$$
$$= v_{xv}\cos(\phi_i + \psi) + v_{yv}\sin(\phi_i + \psi) + \dot{\phi}_i L\sin\psi \qquad (2)$$

On the other hand, the *i*-th active velocity component $v_{ai}$ is a function of the angular velocity of the *i*-th actuator, $\omega_i$, since the ball is driven by the actuator in that active direction. As shown in Figure 1, let $R$ be the radius of the spherical tire and $\alpha$ the angle between the vertical line and the direction of the inclined roller ring. The active velocity $v_{ai}$ is given by

$$v_{ai} = \rho R\sin\alpha \cdot \omega_i \qquad (3)$$

where $\rho$ is the gear reduction ratio associated with the roller ring and the gear of the motor.

Figure 6 shows the whole vehicle with four ball wheels. Frame $O_v$-$X_vY_v$ is attached to the pivotal joint, where the $X_v$ axis is the bisector of the angle between the two beams, $2\phi$. Let $\phi_v$ be the angle of the $X_v$ axis measured from the X axis. The direction of each half beam is given by

$$\begin{aligned} \phi_1 &= \phi_v + \phi, & \phi_2 &= \phi_v - \phi + \pi \\ \phi_3 &= \phi_v + \phi + \pi, & \phi_4 &= \phi_v - \phi \end{aligned} \qquad (4)$$

Our objective is to obtain the relationship between the active ball wheel movements driven by individual actuators and the resultant vehicle motion. To describe the entire vehicle motion including the variable footprint mechanism, four generalized velocities are needed; two translational velocities of the pivotal joint, $v_{xv}$, and $v_{yv}$, angular velocity of the vehicle chassis, $\dot{\phi}_v$, and the time rate of change of the angle between the two beams, $\dot{\phi}$. Substituting eq.(4) into (2) and rotating the coordinate system to the one parallel to the vehicle coordinate system,

$$\begin{bmatrix} v_{a1} \\ v_{a2} \\ v_{a3} \\ v_{a4} \end{bmatrix} = \begin{bmatrix} \cos(\phi+\psi) & \sin(\phi+\psi) & L\sin\psi & L\sin\psi \\ \cos(\phi+\psi) & -\sin(\phi+\psi) & L\sin\psi & -L\sin\psi \\ -\cos(\phi+\psi) & -\sin(\phi+\psi) & L\sin\psi & L\sin\psi \\ -\cos(\phi+\psi) & \sin(\phi+\psi) & L\sin\psi & -L\sin\psi \end{bmatrix} \begin{bmatrix} v_{xv} \\ v_{yv} \\ \dot{\phi}_v \\ \dot{\phi} \end{bmatrix} \qquad (5)$$

For the prototype vehicle to be described later in section 7, the angle of active rolling direction, $\psi$, is 90 degrees, and the above relationship reduces to:

$$\begin{bmatrix} v_{a1} \\ v_{a2} \\ v_{a3} \\ v_{a4} \end{bmatrix} = \begin{bmatrix} -\sin\phi & \cos\phi & L & L \\ -\sin\phi & -\cos\phi & L & -L \\ \sin\phi & -\cos\phi & L & L \\ \sin\phi & \cos\phi & L & -L \end{bmatrix} \begin{bmatrix} v_{xv} \\ v_{yv} \\ \dot{\phi}_v \\ \dot{\phi} \end{bmatrix} \tag{6}$$

The above 4 by 4 matrix in eq.(5) is invertible for all the vehicle configuration, as long as $\cos\phi \sin\phi \neq 0$.

$$\mathbf{V}_v = \mathbf{J}\mathbf{V}_a \tag{7}$$

where

$$\mathbf{V}_v = \begin{bmatrix} v_{xv} & v_{yv} & \dot{\phi}_v & \dot{\phi} \end{bmatrix}^T$$

$$\mathbf{V}_a = \begin{bmatrix} v_{a1} & v_{a2} & v_{a3} & v_{a4} \end{bmatrix}^T$$

$$\mathbf{J} = \begin{bmatrix} \frac{1}{4\cos(\phi+\psi)} & \frac{1}{4\cos(\phi+\psi)} & \frac{-1}{4\cos(\phi+\psi)} & \frac{-1}{4\cos(\phi+\psi)} \\ \frac{1}{4\sin(\phi+\psi)} & \frac{-1}{4\sin(\phi+\psi)} & \frac{-1}{4\sin(\phi+\psi)} & \frac{1}{4\sin(\phi+\psi)} \\ \frac{1}{4L\sin\psi} & \frac{1}{4L\sin\psi} & \frac{1}{4L\sin\psi} & \frac{1}{4L\sin\psi} \\ \frac{1}{4L\sin\psi} & \frac{-1}{4L\sin\psi} & \frac{1}{4L\sin\psi} & \frac{-1}{4L\sin\psi} \end{bmatrix} \tag{8}$$

Note that matrix **J** is the Jacobian relating the vehicle velocity vector to the ball velocities in the active directions. The above analysis shows that the four independent actuators driving the four ball wheels completely determine the vehicle velocity as well as the angular velocity of the footprint reconfiguration mechanism. Note that there is no singular point in the Jacobian and that no over constraint situation occurs in this mechanism.

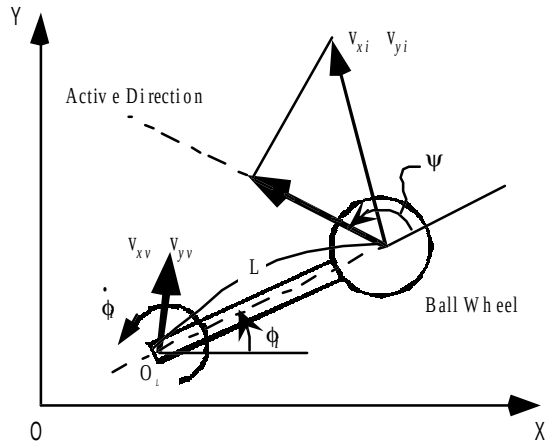


Figure 5: Ball wheel motion

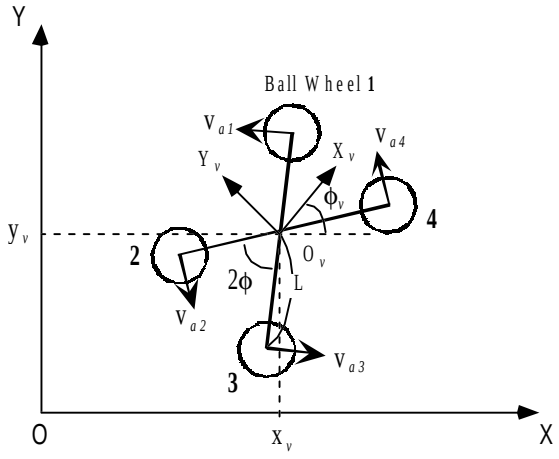


Figure 6: Coordinate system of the vehicle

## 4. Static Stability Augmentation

Static stability is among the most critical requirements for wheelchairs. In this paper, the varying footprint mechanism is used for augmenting the vehicle stability. The objective of static stability augmentation is to keep the position of the mass centroid within the footprint of the platform by varying the joint angle between the two beams. A method for estimating the centroid position and obtaining an optimal joint angle will be presented in this section. Let $m$ be the total inertial load, i.e. the mass of the chair, patient, and vehicle excluding the ball wheels. Let $(x_c, y_c)$ be the coordinates of the mass centroid with respect to the vehicle coordinate frame, as shown in Figure 7. Each ball wheel is equipped with a load cell to monitor the load distribution. Let $F_i$ be the vertical force acting on the $i$-th ball, then the mass centroid position is given by

$$x_c = \frac{L}{mg} F_x \cos\phi \ , \ \ y_c = \frac{L}{mg} F_y \sin\phi \tag{9}$$

where

$$\begin{aligned} F_x &= F_1 - F_2 - F_3 + F_4 \\ F_y &= F_1 + F_2 - F_3 - F_4 \end{aligned} \tag{10}$$

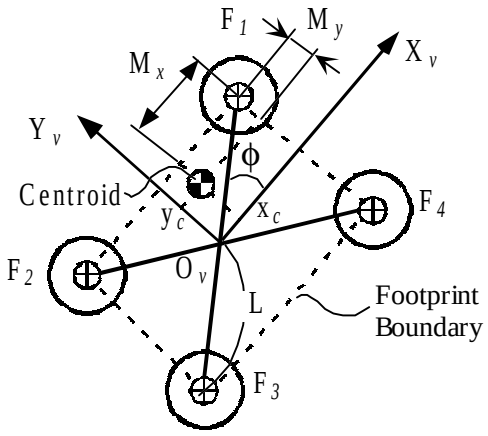


Figure 7: Static stability margin

When the mass centroid is on the boundary of the vehicle footprint shown by the broken lines in the figure, the vehicle is critically stable. Static stability margin is therefore defined to be the minimum distance from the mass centroid position to the footprint boundary. Since the footprint is a rectangular area parallel to the boundary of which is the $X_v$ and $Y_v$ axes, the stability margin can be determined by evaluating the distances to the four sides of the rectangle. Let $M_x$ and $M_y$ be the distances to the boundary in the x and y directions, respectively. As shown in the figure, static stability margin $M$ is given by

$$M = Min(M_x, M_y) \tag{11}$$

where

$$M_x = L\cos\phi - |x_c| \ , \ M_y = L\sin\phi - |y_c| \tag{12}$$

The optimal footprint configuration is then given by the pivotal joint angle that maximizes the static stability margin given above:

$$\phi^0 = \arg \max_{0<\phi<\frac{\pi}{2}} (Min(M_x, M_y)) \tag{13}$$

This is a type of max-min strategy, which best augments the stability in the worst direction. Figure 8 shows the plot of $M_x$ and $M_y$ against $\phi$. The optimal joint angle $\phi^0$ is provided at the intersection of the two curves, $M_x$ and $M_y$. Equating $M_x$ and $M_y$ yields

$$\phi^0 = \tan^{-1} \frac{mg - |F_x|}{mg - |F_y|} \tag{14}$$

The centroid is located in an area where $x_c > 0$, $y_c > 0$, that is the first quadrant of the vehicle coordinate frame, then $F_x > 0$, $F_y > 0$. Therefore the optimal joint angle in the first quadrant is given by

$$\phi^0 = \tan^{-1} \frac{F_2 + F_3}{F_3 + F_4} \tag{15}$$

Optimal angles in other quadrants can be obtained in the same manner. In summary, the optimal angle $\phi^o$ is given by the following form,

$$\phi^0 = \tan^{-1} \frac{Min\{(F_1 + F_4),(F_2 + F_3)\}}{Min\{(F_1 + F_2),(F_3 + F_4)\}} \tag{16}$$

Note that this method does not need the vehicle weight, patient weight and the absolute value of each ball wheel load, but simply needs the ratio of the wheel load distribution.

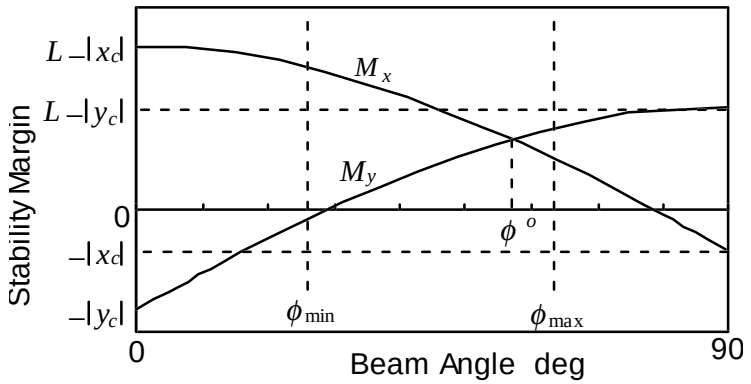


Figure 8: Plot of the static stability margin against the pivotal joint angle

## 5. Transmission Control

Since the Jacobian given by eq.(7) is a function of pivot angle $\phi$, the vehicle velocity varies depending on the footprint configuration, although the individual actuator speeds remain the same. This implies that the varying footprint mechanism would change the kind of transmission ratio between the actuators and the vehicle. In other words, the transmission of the vehicle drive train can be changed from a low gear to a top gear by changing the footprint configuration. Depending on diverse requirements for vehicle speed and traction force, one can change the transmission ratio simply by changing the pivot angle $\phi$. In this section, we will analyze this varying transmission, and discuss its utility.

Suppose that the vehicle is commanded to move forward, i.e. the direction of the X axis. Substituting $v_{xv}$=V, $v_{yv}$=0, $\dot{\phi}_v$=0 and $\dot{\phi}$=0 into eq.(6) yields the velocities of the individual ball wheels in the active rolling direction; $v_{ai}$=-Vsin$\phi$, $v_{a2}$=-Vsin$\phi$, $v_{a3}$=Vsin$\phi$ and $v_{a4}$=Vsin$\phi$. Figure 9 shows these ball wheel velocities and the relationship with the pivot angle $\phi$. Note that the actual ball wheel motion is the vectorial sum of the active rolling driven by the actuator and the passive rolling in the perpendicular direction. As pivot angle $\phi$ decreases, the passive rolling vector becomes longer whereas the active rolling decreases. Therefore the ratio of the vehicle velocity to the active rolling part of the ball wheel velocity increases. This is why the reconfigurable footprint mechanism serves as a variable transmission.

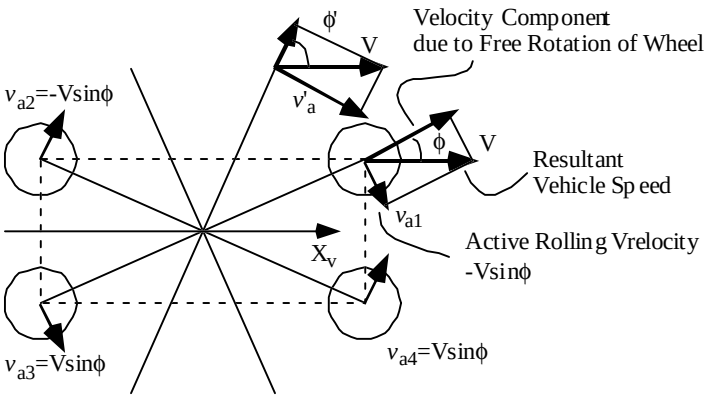


Figure 9 : Kinematics of variable transmission

The above argument on the vehicle transmission ratio in one direction can be extended to that of two-dimensional motion.

Consider the translational part of vehicle motion alone. Translational vehicle velocities $\mathbf{v}_t=[v_{xv}, v_{yv}]^T$ are related to the ball wheel velocity vector $\mathbf{v}_a$ by

$$\mathbf{V}_t = \mathbf{J}_t \mathbf{V}_a \tag{17}$$

where $\mathbf{J}_t$ consists of the first two rows of the Jacobian $\mathbf{J}$.

$$\mathbf{J}_t = \frac{1}{4}\begin{bmatrix} \frac{-1}{\sin\phi} & \frac{-1}{\sin\phi} & \frac{1}{\sin\phi} & \frac{1}{\sin\phi} \\ \frac{1}{\cos\phi} & \frac{-1}{\cos\phi} & \frac{-1}{\cos\phi} & \frac{1}{\cos\phi} \end{bmatrix} \tag{18}$$

The transmission ratio of the vehicle drive system is defined as

$$\lambda = \frac{|\mathbf{V}_t|}{|\mathbf{V}_a|} \tag{19}$$

where $|\mathbf{x}|$ represents the norm of vector $\mathbf{x}$. Note that, since the vehicle is a multi degree-of-freedom system, the standard scalar quotient, i.e. $v_t / v_a$, cannot be used. Therefore, the quotient of the vector norms is used in eq.(19). The rotational transmission ratio can be defined in a form similar to eq.(19). Note, however, that the rotational transmission does not vary depending on the footprint configuration, since the third and fourth rows of Jacobian $\mathbf{J}$ are not functions of pivot angle $\phi$.

The transmission ratio varies depending on the direction of the vehicle motion. The maximum and minimum of $\lambda$ and their directions of motion are obtained from the singular value decomposition of Jacobian $\mathbf{J}_t$.

$$\mathbf{J}_t = \begin{bmatrix}\mathbf{u}_1 & \mathbf{u}_2\end{bmatrix}^T \begin{bmatrix} \frac{1}{2\sin\phi} & 0 & 0 & 0 \\ 0 & \frac{1}{2\cos\phi} & 0 & 0 \end{bmatrix} \begin{bmatrix}\mathbf{v}_1 & \mathbf{v}_2 & \mathbf{v}_3 & \mathbf{v}_4\end{bmatrix} \tag{20}$$

where 1/2sin$\phi$ and 1/2cos$\phi$ are singular values of matrix $\mathbf{J}_t$, and $\mathbf{u}_i$ and $\mathbf{v}_i$ are left and right eigenvectors, respectively. The two singular values provide the maximum and minimum transmission ratios. Namely, for $0< \phi \leq \pi/4$, the transmission ratio takes the maximum, $\lambda_{max}=1/2\sin\phi$, when the vehicle moves in the direction along the corresponding left eigenvector $\mathbf{u}_1^T=[1, 0]$, i.e. the X axis, with the distribution of actuator speeds given by the right eigenvector $\boldsymbol{v}_1^T=[-0.5,-0.5,0.5,0.5]$. The minimum transmission ratio, $\lambda_{min}=1/2\cos\phi$, takes place when the vehicle moves in $\mathbf{u}_2^T=[0, 1]$, i.e. the Y-axis, with the actuator speed distribution of $\boldsymbol{v}_2^T=[0.5,-0.5,-0.5,0.5]$. When the actuator speed distribution is $\boldsymbol{v}_3$ or $\boldsymbol{v}_4$, no translational velocity is generated.

Figure 10 shows the directions of the maximum and minimum transmission ratios, and Figure 11 shows the plot of the max/min transmission ratios against the pivot angle, $\phi$. Note that the transmission ratio varies continuously as pivot angle $\phi$ varies. Therefore, the variable footprint mechanism can be treated as a continuously variable transmission (CVT).

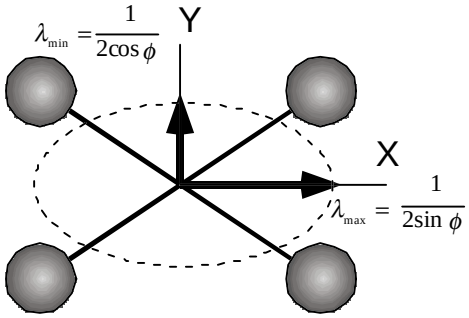


Figure 10: Maximum and minimum transmission ratios

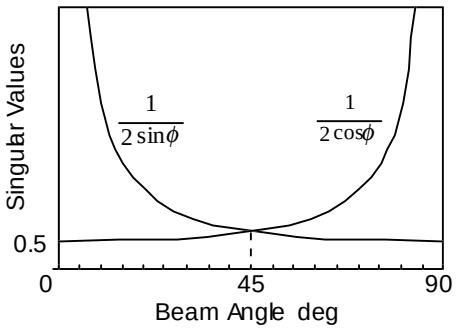


Figure 11: Plots of singular values against beam angle

Note that at $\phi = \pi/4$, the vehicle has an isotropic transmission ratio of $\sqrt{2}/4$ in all directions. Note also that, as the transmission ratio becomes larger, the traction force generated becomes smaller, hence the acceleration of the vehicle becomes smaller. The mechanical advantage is given by the reciprocal of the transmission ratio:

$$MA = \frac{1}{\lambda} = \frac{|\mathbf{F}_t|}{|\mathbf{F}_a|} \tag{21}$$

where $\mathbf{F}_a$ is a 4×1 vector comprising the traction forces at the four ball wheels, and $\mathbf{F}_v$ is the resultant force acting on the vehicle. From the above analysis it follows that

- Pivot angle $\phi$ must be small in order to move at a high speed in the X-direction. For traveling a long distance at a high speed, the footprint should be long in the longitudinal direction.
- For rapid acceleration, the footprint should be shortened in that direction
- Isotropic speed and traction characteristics can be achieved when $\phi = \pi/4$

Three strategies can be used for determining the footprint configuration along with the stability augmentation scheme.

## 6. Control Architecture

As mentioned previously, several kinds of functionality are required to a wheelchair control. Different control modes and control objectives must be selected depending not only on an operator's commands but also on the situations the vehicle is involved. In order to coordinate diverse control modes and objectives, a hierarchical control architecture, similar to a subsumption architecture[7], is used for the system.

To implement the hierarchical architecture, the vehicle behavior has been decomposed into four tasks (A-D) and analyzed to put the priority level to each task.

Task *A* is to move in an arbitrary direction and/or rotate as a operator requests while the vehicle stability is maintained. If the operator does not command to move, the vehicle would stay at a stable location. When the operator requests the vehicle to move by using a joystick, the vehicle would move in a given direction at a given velocity. At the same time in both case, moving or stopping, the footprint configuration would be automatically controlled to maximize the stability margin based on the load distribution among the wheels.

Task *B* is to vary the transmission ratio continuously by changing the pivot angle between the two beams. When the operator commands the vehicle to move at high speed, the footprint configuration would be varied to get a higher gear ratio, narrower configuration, to achieve efficient traveling. The other hand, when larger traction force is needed, the footprint would be varied to get a lower gear ratio, i.e. wider configuration.

Task *C* is going through narrow doorways with the narrowest footprint configuration or to maneuver in crowded area with a footprint configuration which minimizes the rotational radius of the wheelchair. All vehicle motions should be restricted in slow speed during this task. The task *C* would be triggered or reset by the operator's command sent via buttons on the joystick.

Task *D* is preventing falling down of the wheelchair. The static stability margin would be monitored all times and if the margin hits a minimum margin, vehicle movements would be restricted and the footprint configuration would be varied to maintain the minimum stability margin. At the same time, a warning signal would be sent to the operator in order to let him/her aware of the risk.

To build a vehicle control system by using these tasks, a priority order for the hierarchical structure is needed. For an application to a wheelchair, safety is the most important issue to be considered. Considering the importance for safety of each task to give a priority to the task. The most significant problem for a wheelchair is falling down. Falling must be avoided in any situations. To prevent falling, it has to be required that Task *D* can be executed at any moment, if it is needed. Therefore, Task *D* should occupy the highest priority among the tasks. The next serious problem is physical interference between a wheelchair and its environment, i.e. bumps. In the current system, only the operator can recognize the environment around the chair and change the footprint depend on the situations. For example, when going through a narrow doorway, the operator may command to take the narrowest footprint configuration by executing Task *C*. During it moves near the doorway, the footprint must be kept at the configuration except it is changed for prevention of falling. The footprint should not be changed for any other purposes because operator may believe that the footprint keeps a particular shape which he/her commanded. Therefore, Task *C* should have a second higher priority. Task *B*

achieves CVT control which provides additional functionality to Task *A* such as efficient traveling, moving at faster speed and overcoming ramp ways. These are the functions which improve the fundamental mobility required for a wheelchair but does not deal with any safety issues. Task B should have the second lowest priority.

Task *A* is the most fundamental task and minimum requirement for a wheelchair. Therefore Task *A* should be a base layer of the hierarchical control.

These tasks are assigned to four layers(zero-th to 3rd) of the vehicle control system, respectively. The layer of large number has higher priority than that of smaller number, i.e., task *A* occupying the zero-th layer has the lowest priority, and task *D*, occupying the 3rd layer, has highest priority.

The system has hierarchical configuration and would be able to adapt to multiple situations or requirements by changing the layer taking the control. Figure 12 illustrates a schematic of the vehicle control system.

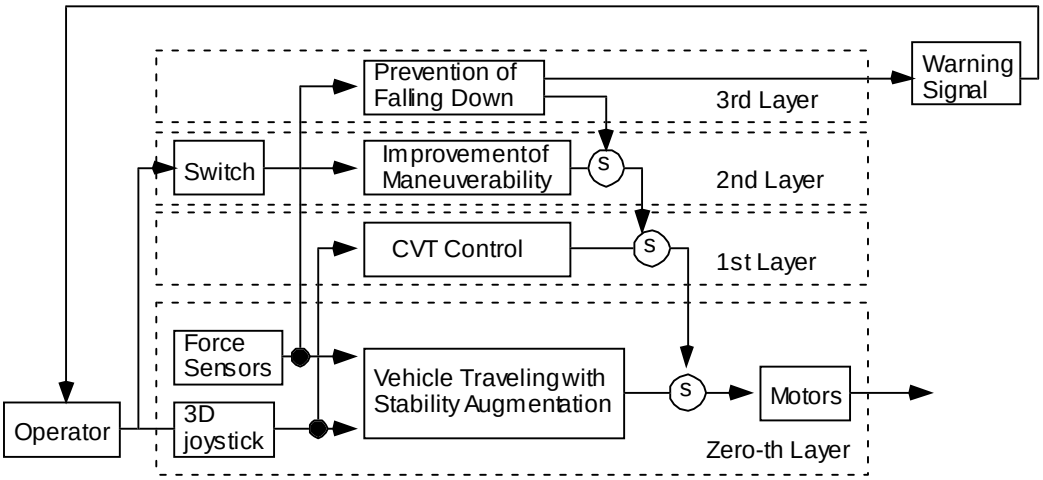


Figure12: Vehicle control system

## 7. Prototyping

A prototype wheelchair with the reconfigurable footprint mechanism has been designed and built. Figure 13 shows the overview of the prototype. All the vehicle drive components, including actuators, ball wheels, and cross beams, are placed beneath the rectangular platform of 510mm wide and 610mm

long. The platform is only 190mm above the floor. A commercially available chair with an aluminium and grass-fiber structure is mounted on the platform. A three degree-of-freedom joystick is attached to one of the arm rests.

Figure 14 shows the bottom view of the prototype wheelchair. The diagonal distance of the footprint, that is, the distance between the floor contact points of the two balls at diagonal positions is 700mm. The joint angle between the two beams varies from 55deg.($\phi_{min}$ = 55/2deg.) to 125deg. ($\phi_{max}$ = 125/2deg.). This means that the wheel base and tread of the vehicle varies between 323mm and 620mm. The absolute angle of the pivotal joint is measured by a potentiometer.

Figure 15 shows a ball wheel unit with an independent suspension mechanism. The ball, 108mm in diameter, is a stainless steel sphere with 3mm thick outer coating of rubber. The oblique roller ring driven by a DC servo motor is arranged in such a way that a traction force is generated in the direction perpendicular to the longitudinal direction of the beam, namely, $\psi$ = 90deg. The suspension mechanism allows the ball wheel to move about 25mm in the vertical direction. A parallelogram mechanism is used for the suspension so that the ball wheel unit may keep the same orientation relative to the vehicle chassis. To minimize the height of the wheel mechanism, coil springs of the suspension are placed horizontally within the parallelogram mechanism. The spring force is transmitted to the top of the ball through a transmission linkage. The vertical load acting on each wheel can be detected by measuring the displacement of the coil spring with a linear potentiometer attached to the side of the spring. Furthermore, an incremental encoder is mounted on each servo motor to measure the ball rotation in its active direction.

Figure 15 shows a differential gear mechanism used for the pivotal joint in order to keep the chair orientation aligned with the bisector of the two beams.

Figure 13: Wheelchair prototype

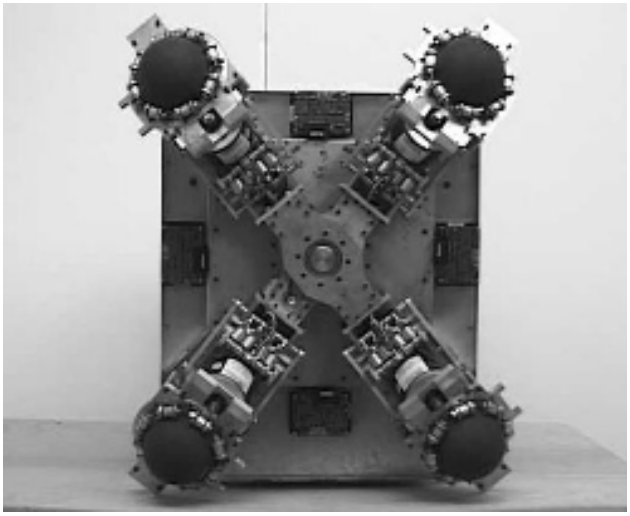

Figure 14: Reconfigurable vehicle (bottom view)

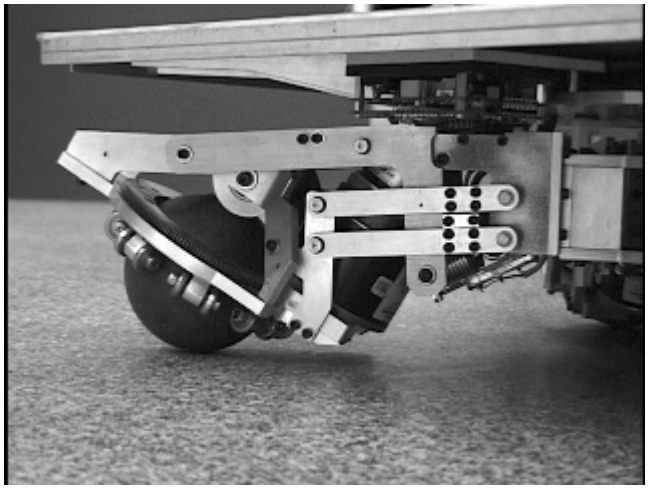

Figure 15: Ball wheel unit

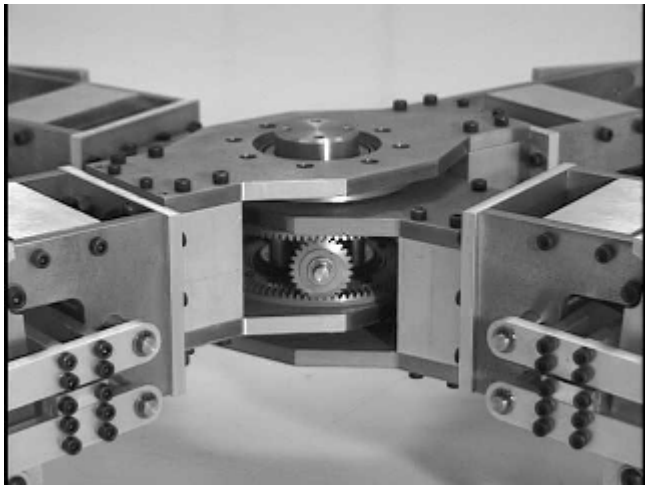

Figure 16: Pivotal joint with differential gears

## 8. Experiments

### 8.1 Kinematics

First the kinematic relationship described by the Jacobian was verified through experiments. The four motors were commanded to move at constant speeds, and the resultant vehicle speed was measured. The experiment was repeated for different footprint configurations. Figure 17 shows one of the experimental results, where each ball wheel speed is kept at 7.5rpm, 15rpm or 22.5 rpm. The

resultant vehicle speed in the x direction varied depending on pivot angle $\phi$. Overall the experimental results agree with the theoretical curves derived from the Jacobian given by eq.(6). Other experiments of vehicle motion in oblique directions and rotational ones showed good agreements with the theoretical Jacobian as well.

**8.2 Static Stability Augmentation**

The stability augmentation algorithm described in section 4 provides the optimal pivot angle that maximizes the stability margin based on the measured distribution of load over the four wheels. As the load shifts to one side, the estimated position of the centroid would move accordingly, and the pivot angle would be changed so as to keep the maximum stability margin. Figure 18 shows the experiments that demonstrates this stability augmentation behavior. A mass of 65kg was applied to the point on the Y axis at distance *L* from the pivotal joint, and the distance *L* increased to increase a moment about the X axis. The actual centroid location, which depends on this load and the mass of the chair itself, shifts a shown by a solid curve in the Figure. The estimated centroid position showed a good agreement with the theoretical curve in most of the load range. Errors in the higher moment range are due to the nonlinearity of the coil springs and the suspension mechanism. The optimal pivot angle started at 45 degree when no moment was applied. As the moment increased, the angle increased to make the footprint wider. When the moment reached 100Nm, the optimal pivot angle hit the upper limit of the angle, $\phi_{max}$=62.5deg, and beyond this point the optimal angle was kept at the upper limit although the centroid position shifted further. As a result, the stability margin decreased more quickly than that in the range where the optimal angle was lower than $\phi_{max}$. Nevertheless, the stability margin did not vanish until the moment reached approximately 300Nm, which is an extraordinary case. In contrast, stability margin vanishes soon when the proposed stability augmentation was not used. As shown in the figure, stability cannot be maintained in a broad range when the footprint configuration is fixed at $\phi$=45deg. This shows a significant advantage of the stability augmentation control implemented on the prototype wheelchair. The vehicle remained stable even when a patient of 100kg in weight fully extended his upper body towards one side of the chair.

### 8.3 Continuously Variable Transmission

The transmission ratio varies about 1.5 times (45 to 27.5deg.) or about 2times (62.5 to 27.5deg.) depend on the footprint configuration as shown in Figure16. This characteristics would be used for the continuously variable transmission (CTV) of the vehicle.

Figure19 shows experimental results of variable transmission control. Figure19(a) shows plots of the pivot angle $\phi$, the vehicle velocity reference $V^*_v$, the actual vehicle velocity $V_v$ and the motor angler velocity $\omega$ when the vehicle changed the velocity with the beam angle fixed at 45degrees; the isotropic configuration. Since the transmission ratio between wheel angler velocity and vehicle velocity is the same all the time, motor torque hit the limit at a certain velocity and the vehicle velocity is saturated at the value. Figure19(b) is the experimental result when the pivot angle $\phi$ was varied by the variable transmission algorithm. Since the direction of vehicle motion which might be given by the operator can not be predicted, the pivot angle should be kept at around the isotropic configuration at zero or slow speed. For this purpose, the reference of the pivot angle larger than 45 degrees given by the variable transmission algorithm would be ignored, i.e., the layer of this algorithm does not take control.

By means of the variable transmission control, both the wheel angler velocity $\omega$ and the pivot angle $\phi$ are varied continuously and smoothly. As a result, the maximum vehicle velocity has been increased about 15% higher than that achieved by the isotropic footprint configuration.

The other hand, varying the footprint configuration can also change the traction force between ball wheels and the ground. Large traction force is needed not only for getting high accelerations or decelerations but also for climbing up ramps. The small traction force would restrict the vehicle to go through steep ramps in crowded area, especially in the residential homes. The wider footprint configuration in lateral direction allows the vehicle to provide the larger traction force. Figure 20 is the photo of the wheelchair climbing up a 10degrees' ramp. Table 1 shows the experimental result of going up ramps with various footprint configurations. "O" indicates the wheelchair successfully climbing up the ramp and "X" indicates the failure. The prototype wheelchair could climb up 12.5 degrees' ramp with the wider configuration, $\phi$=62deg. This allows the wheelchair to ride on a low-floor van without any powered lifting mechanism.

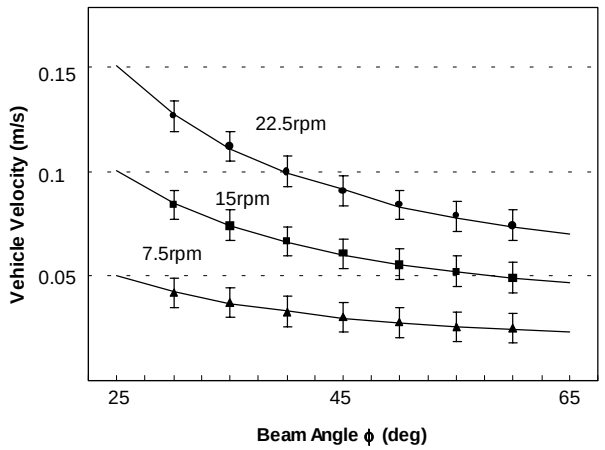


Figure 17: Vehicle velocities against beam angle

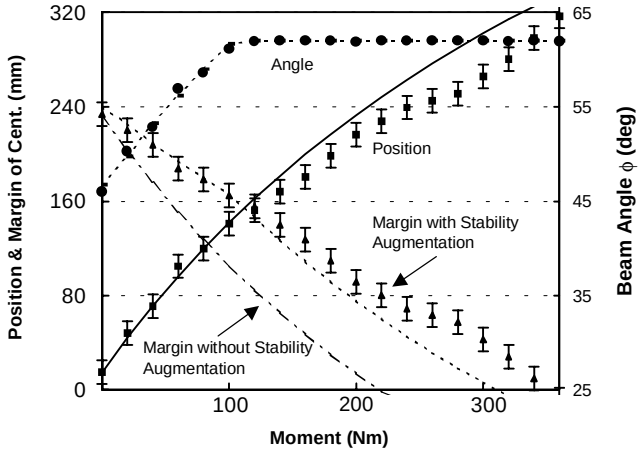


Figure 18: Stability augmentation control

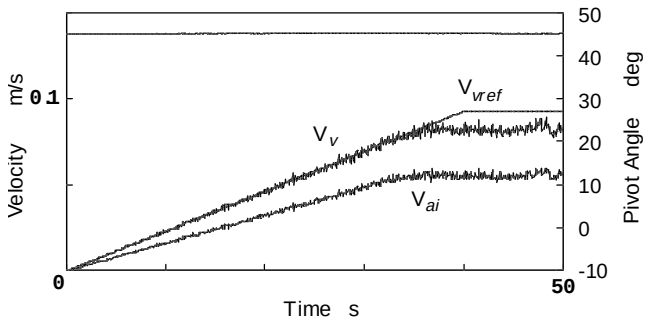


(a) Fixed at isotropic beam angle($\phi$ = 45deg)

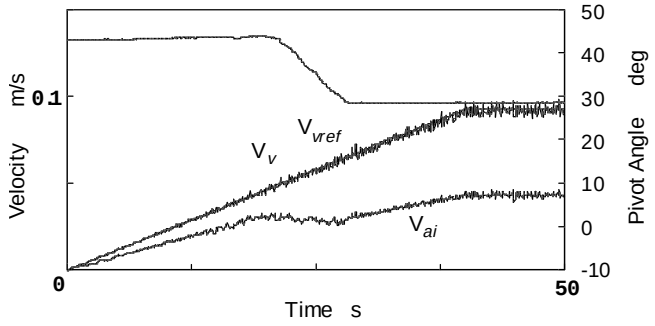


(b) With continuously variable transmission

Figure 19 : Variable transmission control

Figure 20 : Wheelchair climbing up a 10degrees' ramp

Table 1 : Limit angle of the ramp along the vehicle footprint configuration

| Inclination of Ramp (deg.) \ Footprint Configuration $\phi$ (deg.) | 28 | 36.5 | 45 | 53.5 | 62 |
|---|---|---|---|---|---|
| 2.5 | O | O | O | O | O |
| 5 | X | O | O | O | O |
| 7.5 | X | X | O | O | O |
| 10 | X | X | O | O | O |
| 12.5 | X | X | X | X | O |
| 15 | X | X | X | X | X |

## 9. Conclusion

A new mechanism for varying footprint for a four wheeled holonomic omnidirectional vehicle has been proposed and applied to a mobile platform of a wheelchair. A reconfigurable mechanism consists of two beams has been developed and the kinematic model has been obtained. An extra 1DOF for varying footprint not only provides an additional functionality to the vehicle but also solves an over constraint problem of four wheeled vehicles. The vehicle's 4DOF including a freedom of the reconfiguration of the footprint can be controlled independently by four motors driving ball wheels, i.e., driving the four ball wheels allow the vehicle to move in an arbitrary direction with an arbitrary angular velocity and change the footprint configuration at the same time. Then we have established a stability augment control algorithm, variable transmission algorithm and footprint shape control based on the proposed reconfigurable mechanism. Tasks required to the wheelchair with reconfigurable mechanism have been decomposed, analyzed and coordinated by the subsumption control architecture. These control methods has been implemented to a wheelchair prototype. Experimental results using the prototype have shown augmentation of the stability, smooth changing the transmission ratio and providing the large traction force of the wheelchair. These different tasks are coordinated by the subsumption architecture and share the vehicle control properly depending on situations of the wheelchair and requirements of an operator.

## References


[1] H.P.Moravec, Ed., : “Autonomous Mobile Robots Annual Report - 1985,” Robotics Institute Technical Report, Carnegie Mellon University, Pittsburgh, PA. , 1986.

[2] U. Borgolte, et al. : “Intelligent Control of a Semi-Autonomous Omnidirectional Wheelchair,” Proc. of the 3rd International Symposium on Intelligent Robotic Systems `95 (SIRS `95), 1995.

[3] M. Gerke and H. Hoyer : “Planning of Optimal Paths for Autonomous Agents Moving in Inhomogeneous Environments,” 8th Int. Conference on Advanced Robotics (ICAR97), July 1997

[4] F.G.Pin and S.M.Killough : “A New Family of Omni-directional and Holonomic Wheeled Platforms for Mobile Robots,” IEEE Transactions on Robotics and Automation, Vol.10, No4, pp480-489, 1994

[5] M.West and H.Asada : “Design of a Holonomic Omnidirectional Vehicle,” 1992 IEEE Int. Conf. on Robotics and Automation, pp97-103, May.1992.

[6] S.Hirose and S.Amano : “The VUTON : High Payload High Efficiency Holonomic Omni-Directional Vehicle,” 6th Int. Symp. on Robotics Research, October.1993.

[7] M.West and H.Asada : “Design and Control of Ball Wheel Omnidirectional Vehicles,” 1995 IEEE Int. Conf. on Robotics and Automation, pp1931-1938, May.1995.

[8] S.Mascaro, J.Spano and H.Asada : “A reconfigurable Holonomic Omnidirectional Mobile Bed with Unified Seating (RHOMBUS) for Bedridden Patients,” 1997 IEEE Int. Conf. on Robotics and Automation, pp1277-1282, April.1997.